CHEMICAL ENGINEERING TRANSACTIONS
VOL. 38, 2014
A publication of AIDIC
The Italian Association of Chemical Engineering
www.aidic.it/cet
Guest Editors: Enrico Bardone, Marco Bravi, Taj Keshavarz

ISBN 978-88-95608-29-7; **ISSN** 2283-9216
DOI: 10.3303/CET1438009

Hydrodynamics of a Model Stirred Anaerobic Digester

Giuseppina Montante[a*], Alessandro Paglianti[b]

[a]Department of Industrial Chemistry "Toso Montanari", University of Bologna, via Terracini 28, 40131 Bologna, Italy
[b]Department of Civil, Chemical, Environmental and Materials Engineering, University of Bologna, via Terracini 28, 40131 Bologna, Italy
giuseppina.montante@unibo.it

The aim of this work is to identify the hydrodynamic characteristics of a model bioreactor, whose geometrical configuration is adopted at industrial scale for the biomethanation of agricultural scraps. The laboratory scale model bioreactor is a flat bottomed, unbaffled, cylindrical tank of small aspect ratio, centrally stirred by two Lightnin A310 axial impellers. It results from the scale-down of a full-scale design, adopting the geometrical similarity criterion. The Particle Image Velocimetry (PIV) technique is adopted in order to gain a detailed description of the single phase velocity field. The results collected at various impeller rotational speeds and two fill ratios are presented and the effect of the different operating conditions on the model digester hydrodynamics are identified. The experimental characterization allows to assess the appropriateness of the design to achieve an appropriate liquid flow pattern, which ultimately affects the solid feedstock suspension and distribution all over the vessel volume. Finally, possible geometrical modifications for improvements of the overall mixing operation are suggested.

1. Introduction

Stirred anaerobic digesters are increasingly adopted for the conversion of industrial and agricultural organic wastes into biogas by wet or dry fermentation processes. The capability to cope the requirement of renewable energy production and efficient waste treatment makes the so-called bio-methanation a very attractive process (Lv et al., 2010). Different anaerobic digestion operations have been investigated so far, ranging from the co-digestion of waste activated sludge with organic wastes (Cavinato et al., 2010) to the dry digestion of fruit and vegetable wastes (Babaee and Shayegan, 2011) and the fermentation of winery wastes (Colussi et al., 2012), just to mention a few examples.
Among several other factors, the fluid dynamic characteristics of the digesters affect the technical and economical feasibility of bio-methanation. The importance of accounting for the mixing conditions, which are mainly provided by mechanical agitation (Low et al., 2012), has been already shown in several works so far (e.g. Karim et al., 2005; Terashima et al., 2009).
The industrial digesters often operate with dense solid-liquid suspensions, whose physical characteristics experience variation during the fermentation process (O'Neil, 1985).
Typically, for domestic sewage and agricultural manure feedstocks, the solid-liquid mixture in the digesters is modelled as a non-Newtonian liquid phase (Craig et al., 2013), while the two-phase nature of the mixtures should be accounted for in the case of agricultural and forest scraps, whose physical characteristics might give rise to significant sedimentation and flotation behavior. In these cases, the particle size has been shown to affect the biogas production (Sharma et al., 1988), thus leading to suggest the residues gridding as a pretreatment before the digestion.
In all cases, a detailed fluid dynamic analysis of the bioreactor can provide useful information for moving a step toward the improvement of bioslurry systems, which are often operated on the basis of an empirical approach (Tamburini et al., 2012), mitigation of well know operational problems, such those due to swelling and foaming of the digestate (Kowalczk et al., 2013), and optimization of energetic requirements.
In this work, the single phase flow of a Newtonian fluid in a typical digester geometrical configuration is considered, provided that worsening of the mixing features can be expected at higher liquid viscosity and with the addition of the solid feedstock to be digested.

Please cite this article as: Montante G., Paglianti A., 2014, Hydrodynamics of a model stirred anaerobic digester, Chemical Engineering Transactions, 38, 49-54 DOI: 10.3303/CET1438009

2. Experimental

The investigated model bioreactor was a cylindrical vessel with a flat bottom made of Perspex and closed with a lid on top. The vessel diameter, T, was equal to 0.49m and the height, H, was equal to T/2. As a difference with the stirred tanks adopted in most biotechnological applications, it was not provided with baffles. Mixing was achieved by two identical Lightnin A310 impellers of diameter, D, equal to 0.2T, mounted on the same shaft coaxially with respect to the vessel axis. The lower impeller was placed at an off-bottom clearance, C1, equal to 0.08T and at a distance from the upper impeller, C2, equal to 0.18T. A schematic representation of the stirred vessel with the indication of the main geometrical parameters is reported in Figure 1. As the model liquid, demineralised water was adopted. Different liquid levels, H_L, were considered, i.e. H_L=H, H_L=0.76H and H_L=0.6H, this last being the closer to the scale-down condition. As for the impeller rotational speed, N, it was varied from 100rpm up to the value corresponding to the onset of vortex ingesting, which depends on the liquid level.

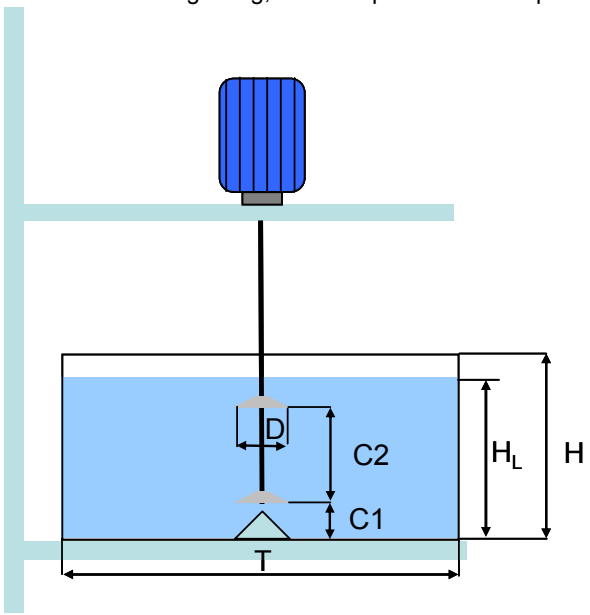

Figure 1. Main geometrical characteristics of the mode bioreactor.

The ensemble-averaged flow field was determined by the PIV technique already adopted for the fluid dynamic characterization of a bio-hydrogen fermenter (Montante et al., 2013). The data were collected on a diametrical vertical plane of the vessel, thus obtaining the axial and radial components of the velocity vector. A view of the measurement system arrangement is shown in Figure 2. It included a Litron Nd:YAG laser, emitting light at 532 nm with a maximum frequency of 15 Hz and energy equal to 65mJ, and an HiSense MK II, 1344×1024 pixels CCD camera. Polymeric particles coated with fluorescent Rhodamine B emitting light at the wavelength of 590 nm were selected for seeding the fluid. The camera was provided with a low pass optical filter cutting the light wavelength lower than that of the fluorescent seeding particles emission. To minimize refraction effects at the curved surface, the vessel was placed inside a square tank filled with the working liquid. The thickness of the laser sheet, the time interval between two laser pulses, the number of samples and the overall extend of the measurements were set after a careful error evaluation. The PIV parameters setting procedure was found to be particularly tough for the present geometry with respect to standard configurations, due to the strong variations of the velocity magnitude moving from the impeller region towards the vessel wall, to the flow instabilities appearance and to the highly tangential fluid motion typical of unbaffled tanks (Busciglio et al., 2011).
As for the time interval between two laser pulses, Δt, in order to keep particles displacement below 25% of the interrogation area length, L_{IA}, the following criterion was adopted (Raffel et al. 1998):

$$\Delta t = \frac{0.25 L_{IA} S}{Vtip} \tag{1}$$

Where S is the object to image scale factor and V_{tip} is the impeller tip speed, defined as:

$$V_{tip} = \pi ND \tag{2}$$

Also the relationship between Δt and the laser sheet thickness, z_l, to account for the through-plane motion of the particle was considered:

$$\Delta t = \frac{0.25 z_l}{W} \tag{3}$$

where W is the tangential velocity component, that in the proximity of the impellers can be assumed close to V_{tip}. .
Following Gomez et al. (2010) and considering that significant velocity magnitude variations are expected due to the small height to diameter ratio of the vessel, a relaxed V_{tip} value was considered when applying the above mentioned well-established criteria. Finally, based on Eqn. (3) and adopting a reduction factor of 50% for V_{tip}, the time interval between two laser pulses was varied in the range 500-1500 μs, depending on the impeller speed. The laser thickness in the measurement region was equal to 1.5mm.
The following procedure was adopted for obtaining the instantaneous and ensemble averaged velocity vectors from the raw image pairs: a cross-correlation algorithm to each image pair on a rectangular grid with 50% overlap between adjacent cells and an interrogation area of 32×32 pixel was applied, the instantaneous vectors were submitted to a validation procedure based on the evaluation of the peak heights in the correlation plane and of velocity magnitude. At least 1000 image pairs were required to obtain statistical convergence on mean velocities, while for selected conditions the mean velocity was calculated over 6000 instantaneous values. The vector grid was of about 2.5mm × 2.5mm.

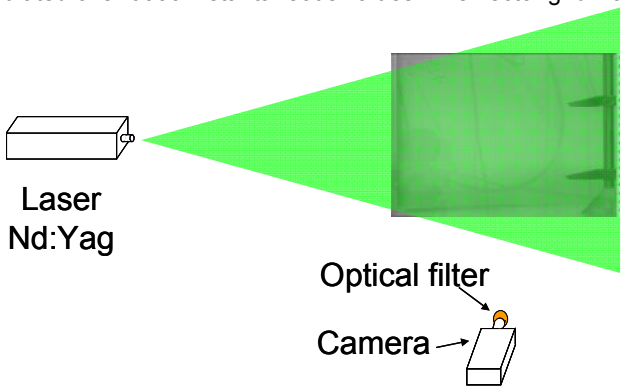

Figure 2. Arrangement of the PIV system.

3. Results and Discussion

The preliminary visual observation of the stirred tank has shown that the fluid dynamic steady state condition is achieved after a very long transient from the agitation onset. The time extend of the transient depends on the impeller speed and the fill ratio, but in any case tens of minutes from the agitation onset are required, while typical values for stirred tanks are tens of seconds (e.g. Brown et al., 2004). Also, for selected conditions, wide liquid free surface oscillations take place after at least 30 minutes from the agitation onset, as can be observed in the two subsequent snapshots of the vessel shown in Figure 3, where together with the different position of the liquid free surface, the central vortex is also tracked.
Based on these visual observation, all the PIV data shown in the following were collected after at least 30 minutes from the agitation onset.
The ensemble averaged velocity field normalized by V_{tip} over 1000 instantaneous measurements on a vertical diametrical plane obtained at H_L=H and different rotational Reynolds numbers are shown in Figure 4. The results show that the impeller action is significant up to r/T=0.20, while going towards the vessel lateral wall the liquid velocity decreases of one order of magnitude with respect to the impeller discharge region. It is worth observing that above the upper limit of the impeller speed adopted in the experiments (i.e. N=422rpm, corresponding to $Re=6.6\times10^4$) gas ingestion from the central vortex took place. A scrutiny of the specific flow features close to the vessel bottom shows that the velocity vectors are directed towards the vessel centre probably due to the inclination of bottom impeller discharge flow, which does not reach

the vessel base. Also, the flow field does not scale exactly with the impeller tip speed, as usually happens in turbulent single phase flow stirred tanks. On the other end, as recently pointed out by Machado et al. (2013), to keep the flow turbulent in the whole vessel volume, the rotational Reynolds number should be much higher than that ensuring the turbulent regime close to the impeller.

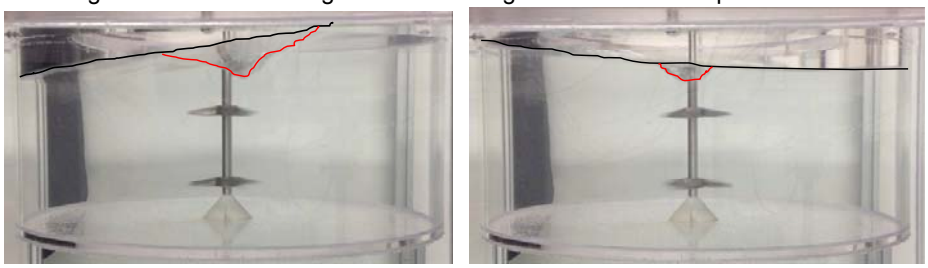

Figure 3. Snapshots of the vessel working under unstable conditions. Red line: vortex profile; black line: free liquid surface.

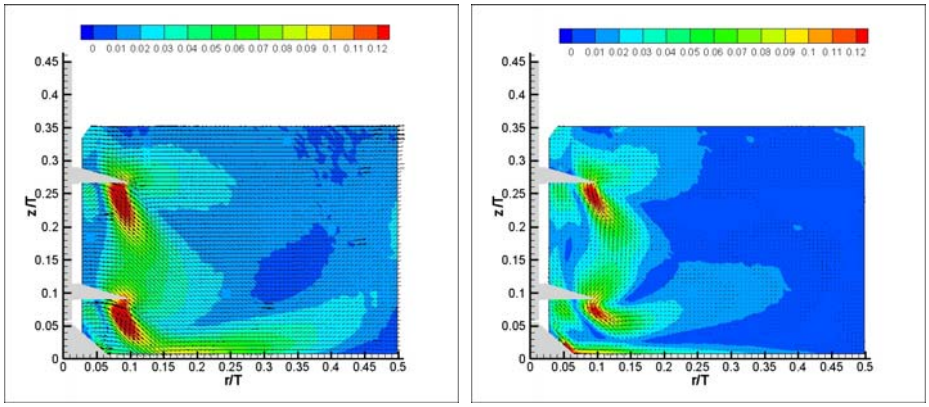

Figure 4. The ensemble averaged velocity field at different Reynolds number, H_L=H.

Considering the long transient time before the achievement of pseudo-steady state conditions and the apparent unstable motion visually observed for selected combinations of operating conditions, the effective time independency of the ensemble average flow field shown in Figure 4 was further verified, by extending the acquisition to 6000 image pairs and calculating the ensemble average of 1000 instantaneous velocity fields at different time distance from the acquisition onset. An example of the results is shown in Figure 5. The comparison of the velocity maps confirms that the selected measurement parameters allow to obtain a meaningful ensemble averaged flow field.

As for the effect of the fill ratios, the results obtained for H_L=0.76H at different Reynolds numbers are shown in Figure 6. The change of the qualitative features of the impeller discharge flow is apparent and the variation of the ensemble averaged mean velocity field with V_{tip} (or Re) is more marked than for H_L=H. A further decrease of the liquid level (H_L=0.60H) dramatically reduces the upper impeller pumping action and the shape of both the impeller discharge flows are again different with respect to the other investigated conditions, as can be observed in Figure 7.

Overall, a strong dependency of the mean velocity field on the impeller speed and on the liquid level is found and in all cases in wide portions of the reactor the fluid is almost stagnant. Due to the characteristics of the single-phase flow, it may be argued that the suspension of a solid feedstock in the present geometrical configuration is hardly achievable, even at higher impeller speeds.

A possible simple modification to the current geometry is the adoption of the eccentric agitation, that is a viable alternative to baffling. Improvements of the impellers pumping action and of the turbulent parameters can be obtained by off-centering the impeller shaft with respect to the vessel axis, as demonstrated by further experimental investigation, that will be discussed in future works.

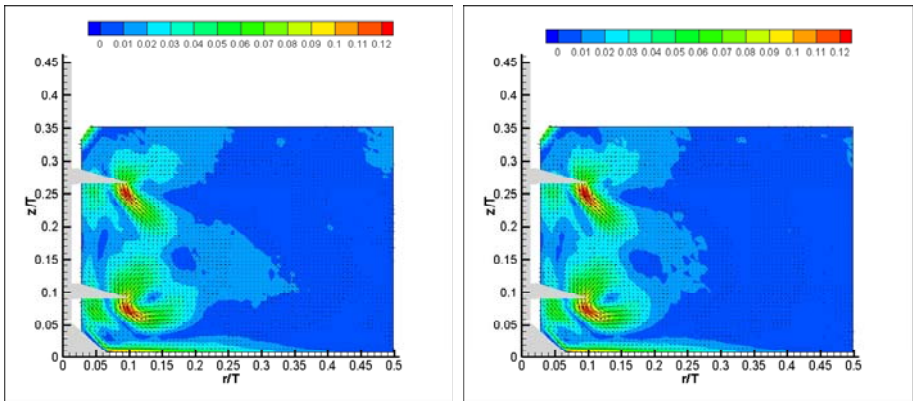

Figure 5. The ensemble averaged velocity field at different time from the acquisition start. Re=6.6×10^4, H_L=H.

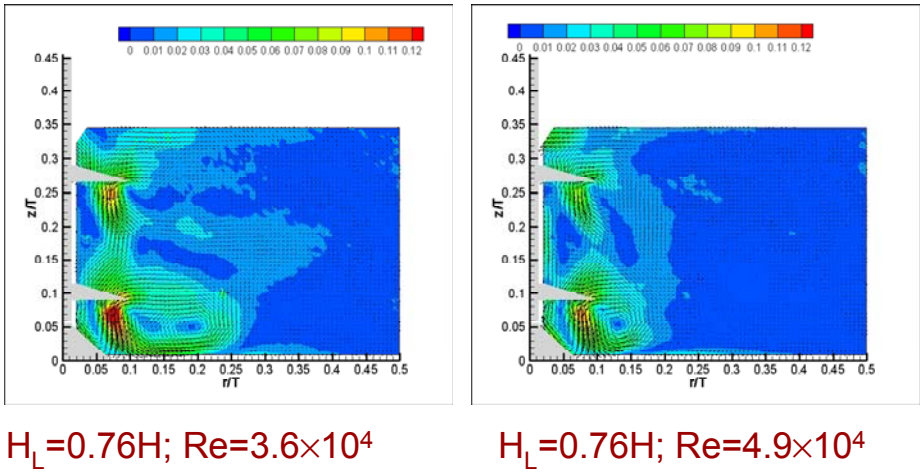

Figure 6. The ensemble averaged velocity field at different Reynolds number, H_L=0.76H.

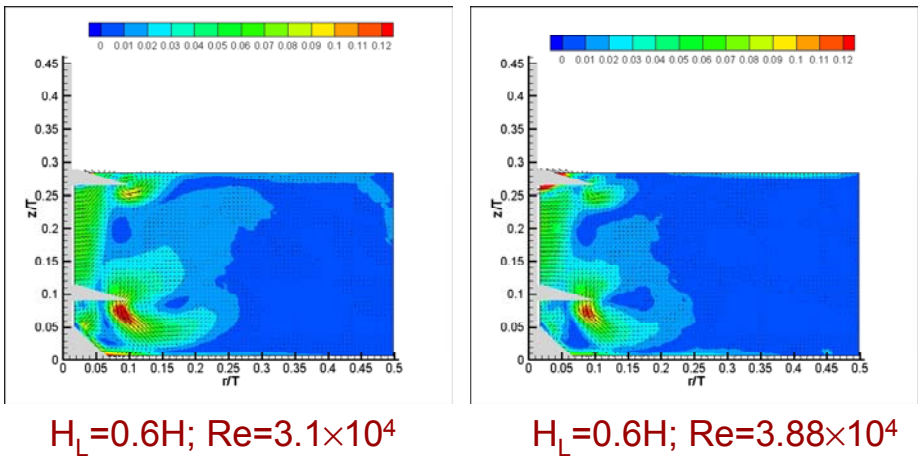

Figure 7. The ensemble averaged velocity field at different Reynolds number, H_L=0.6H.

4. Conclusions

The present fluid dynamic investigation has allowed to identify a number of critical fluid dynamics characteristics of the investigated model digester. The liquid phase velocity field was found to be strongly dampened far from the impellers region, thus leading to wide stagnant zones. As a difference with the case of conventional stirred tanks operating in fully turbulent regime, for this reactor configuration long transient for achieving the steady state conditions are required, moreover, the shape of the discharge flows of the impellers and their interactions are significantly affected by the specific impeller speed. Under particular conditions, free surface instabilities of wide amplitude take places.
Overall, the results show that this widely adopted digester configuration is not optimized even for the simple case of Newtonian fluid mixing, therefore improvement of the overall biogas production operation might be expected by selecting modified agitation configurations.

References

Babaee A., Shayegan J., 2011, Anaerobic digestion of vegetable waste, Chemical Engineering Transactions 24, 1291-1296, DOI: 10.3303/CET1124216.

Brown D.A.R., Jones P.N., Middleton J.C., 2004. Experimental Methods. Chapter 4 in: “Handbook of Industrial Mixing: Science and Practice”, Paul, E.L., Atiemo-Obeng, V.A., Kresta, S.M., Eds, Wiley-Interscience: Hoboken, NJ., pp 183-184.

Busciglio A., Grisafi F., Scargiali F., Daví M.L., Brucato A., 2011, Vortex shape in unbaffled stirred vessels: Experimental study via digital image analysis 2011. Chemical Engineering Transactions 24, 1387-1392, DOI: 10.3303/CET1124232.

Cavinato C., Fatone F., Bolzonella D., Pavan P., 2010, Mesophilic to thermophilic conditions in codigestion of sewage sludge and OFMSW: Evaluation of effluent stability using Dynamic Respirometric Index (DRI) and Biochemical Methane Potential (BMP), Chemical Engineering Transactions 20, 175-180.

Colussi I., Cortesi A., Gallo V., Rubesa Fernandez A.S., Vitanza R., 2012, Modelling of an anaerobic process producing biogas from winery wastes, Chemical Engineering Transactions 27, 301-306, DOI: 10.3303/CET1227051.

Craig K.J., Nieuwoudt M.N., Niemand L.J., 2013, CFD simulation of anaerobic digester with variable sewage sludge rheology, Water Research 47, 4485-4497.

Gómez C., Bennington C.P.J., Taghipour F., 2010, Investigation of the flow field in a rectangular vessel equipped with a side-entering agitator, Journal of Fluids Engineering, Transactions of the ASME 132, 0511061-05110613.

Karim K., Hoffmann R., Klasson T., Al-Dahhan M.H., 2005, Anaerobic digestion of animal waste: Waste strength versus impact of mixing, Bioresour. Technol. 96, 1771-1781.

Kowalczyk A., Harnisch E., Schwede S., Gerber M., Span R., 2013, Different mixing modes for biogas plants using energy crops, Appl. Ener. 112, 465-472.

Low S.C., Parthasarathy R., Slatter P., Eshtiaghi N., 2012, Hydrodynamics study of sludge in anaerobic digesters, Chemical Engineering Transactions 29, 1321-1326, DOI: 10.3303/CET1229221.

Lv W., Schanbacher F.L., Yu Z., 2010, Putting microbes to work in sequence: Recent advances in temperature-phased anaerobic digestion processes, Bioresour. Technol. 101, 9409-9414.

Machado M.B., Bittorf K.J., Roussinova V.T., Kresta S.M., 2013, Transition from turbulent to transitional flow in the top half of a stirred tank, Chem. Eng. Sci. 98 , 218-230.

Montante G., Magelli F., Paglianti A., 2013, Fluid-dynamics characteristics of a vortex-ingesting stirred tank for biohydrogen production, Chem. Eng. Res. Des. 91, 2198-2208.

O'Neil D.J., 1985, Rheology and mass/heat transfer aspects of anaerobic reactor design, Biomass 8, 205-216.

Raffel M., Willert C., Kompehans J., 1998, Particle Image Velocimetry. A Practical Guide. Experimental Fluid Mechanics, Springer, Berlin, Germany.

Sharma S.K., Mishra I.M., Sharma M.P., Saini J.S., 1988, Effect of particle size on biogas generation from biomass residues Biomass 17, 251-263.

Tamburini A., Cipollina A., Micale G., Brucato A., 2012, Measurements of Njs and power requirements in unbaffled bioslurry reactors, Chemical Engineering Transactions 27, 343-348, DOI: 10.3303/CET1227058.

Terashima M., Goel R., Komatsu K., Yasui H., Takahashi H., Li Y.Y., Noike T., 2009, CFD simulation of mixing in anaerobic digesters, Bioresour. Technol. 100, 2228-2233.